

# An Attention Mechanism for Robust Multimodal Integration in a Global Workspace Architecture

Roland Bertin-Johannet, Lara Scipio, Leopold Maytié, Rufin VanRullen  
 Univ. Toulouse, CNRS, CerCo; ANITI, Artificial and Natural Intelligence Toulouse Institute  
 Toulouse, France

**Abstract**—Global Workspace Theory (GWT), inspired by cognitive neuroscience, posits that flexible cognition could arise via the attentional selection of a relevant subset of modalities within a multimodal integration system. This cognitive framework can inspire novel computational architectures for multimodal integration. Indeed, recent implementations of GWT have explored its multimodal representation capabilities, but the related attention mechanisms remain understudied. Here, we propose and evaluate a top-down attention mechanism to select modalities inside a global workspace. First, we demonstrate that our attention mechanism improves noise robustness of a global workspace system on two multimodal datasets of increasing complexity: Simple Shapes and MM-IMDb 1.0. Second, we highlight various cross-task and cross-modality generalization capabilities that are not shared by multimodal attention models from the literature. Comparing against existing baselines on the MM-IMDb 1.0 benchmark, we find our attention mechanism makes the global workspace competitive with the state of the art.

**Index Terms**—Neural Networks, Attention, Global Workspace Theory, Multimodal Fusion, Noise Robustness

## I. INTRODUCTION

*Note : This work has been submitted to the IEEE for possible publication. Copyright may be transferred without notice, after which this version may no longer be accessible.*

In Multimodal machine learning, robustness to missing or degraded modalities is a central open problem [1]–[3]: will the trained systems work in real-world scenarios, where sensors may fail and data may be corrupted or even missing [4]–[6]? In practice, to solve the robustness problem, one is often forced to choose between scaling large end-to-end systems that demand vast amounts of data, training, and deployment budgets [7], [8], or using smaller fusion mechanisms (e.g., gating- and attention-based fusion) that must be retrained whenever the downstream task or available modalities change.

Existing approaches in this category span a range of fusion mechanisms: gated units such as GMU use multiplicative gates to modulate each modality’s contribution to a shared representation [9]; cross-modal attention architectures such as MuLT rely on directional pairwise attention to transfer information between modality streams [10]; dynamic methods such as DynMM use a gating function to select between uni- and multimodal experts (or fusion operations), yielding data-dependent computation paths [11]. Despite these differences, such models typically learn representations and fusion jointly in end-to-end systems, so the specific role of the selector is hard to isolate—it is unclear how much robustness is due to the controller itself versus the representations it co-adapts with.

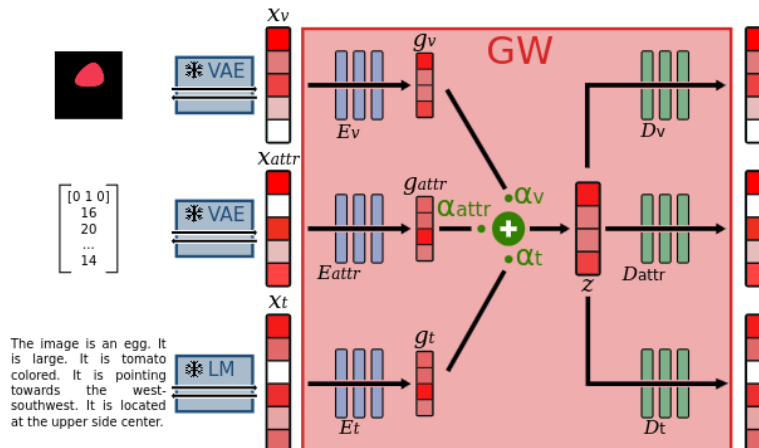
We argue that Global Workspace Theory (GWT) [12]–[14] offers a potential resolution to this problem. GWT proposes that specialized brain systems (vision, language, motor control, memory, etc.) coordinate via a shared, capacity-limited “global workspace” rather than through dense pairwise communication. Information is translated from the specialist modules into an amodal workspace representation, and an attentional mechanism acts as a spotlight that selects which source(s) can write to it before the result is broadcasted back to the specialists.

Several works take inspiration from GWT to improve multimodal systems. In general, they introduce GW-inspired shared bottlenecks or agents for multimodal processing and representation learning [15]–[21]. Yet, again, these fusion schemes entangle attention with representation learning in end-to-end networks, so the specific role of the selector is hard to isolate. From GWT, we predict that a small controller on top of a frozen multimodal workspace could flexibly re-weight modalities under changing reliability conditions, without retraining the whole system. A minimal, modality-wise selector studied under controlled, modality-specific corruptions therefore provides a clean testbed for how much robustness and transfer can be delegated to such a GW-style attention mechanism.

Here, we deliberately focus on static, paired multimodal data (instead of dynamic input sequences like video streams). This ensures changes in performance can be attributed to the attention mechanism itself, rather than to sequence modeling or cross-time alignment. Within this controlled regime, we study how a workspace-based selector enables robust multimodal integration on an official benchmark (MM-IMDB 1.0), how it behaves in the presence of noise or modality corruptions, and how well it transfers across tasks and modalities.

In this work, we build directly on the global latent workspace (GLW) framework of [22], which learns an amodal latent space between pretrained, frozen modules using translation, demi-cycle, cycle and contrastive objectives (defined below). In their original setup, each training step encodes a single modality into the workspace and decodes into one other modality, so the GLW cannot fuse multiple inputs at once. We solve this issue by adding a fusion mechanism, which also allows many-to-many rather than one-to-one broadcast, influencing the training of the GLW representation itself. On top of this pretrained multimodal workspace, we introduce a small, modality-wise attention mechanism that:

**A**



**B**

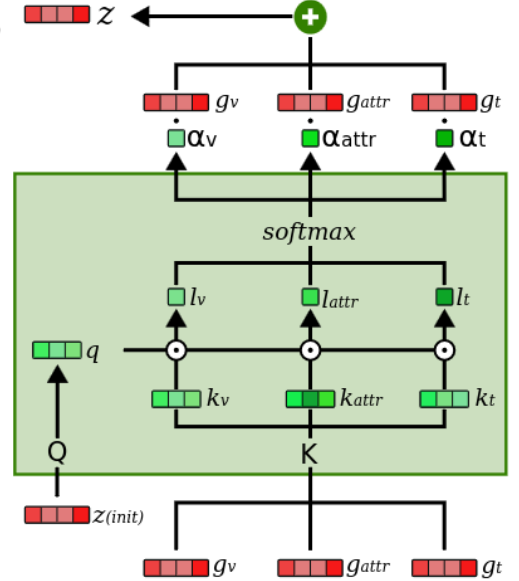


Fig. 1. Proposed architecture (illustrated for the Simple-Shapes dataset). **A** : GW multimodal representation model. Reading from left to right, we start with raw data (images, text, attribute vectors), encoded through modality-specific backbones, pretrained and frozen during GW learning. We project the modality-specific latents  $X_i$  to amodal GW representations  $g_i$  with MLP encoders  $E_i$ . These latent representations are then fused with a weighted average to produce a single vector  $z$  (the role of the attention mechanism will be to set these weights  $\alpha_i$ ). The GW representation  $z$  can then broadcast back to the modality-specific latent spaces using GW decoders  $D_i$ . The GW encoders and decoders are pretrained with randomly chosen attention weights on each data sample. **B** : Our attention mechanism computes modality weights  $\alpha_i$  from an initial fused GW latent  $z^{(init)}$ . We start from the pre-fusion GW latents  $g_i$  and form  $z^{(init)}$  by uniform fusion (equal weights) across modalities. A single shared Key matrix  $K$  produces keys  $k_i$  from each  $g_i$ , and a Query matrix  $Q$  produces a query  $q$  from  $z^{(init)}$ . We then compute  $\alpha_i$  via dot products  $\langle q, k_i \rangle$  followed by a softmax across modalities. These weights define the final attention-weighted fusion that yields the GW latent  $z$ .

- learns modality selection from structured per-modality noise while keeping the global workspace and task probes frozen, both on the Simple Shapes dataset with synthetic noise and on MM-IMDb with realistic corruption
- yields higher corruption robustness than baselines from the literature on a  $20\text{--}25\times$  smaller parameter budget
- transfers its learned selection strategy to unseen downstream tasks, and even to an unseen modality, without any finetuning
- is competitive with state-of-the-art [23] on the MM-IMDb 1.0 benchmark at substantially lower pretraining FLOPs.

We will make our data/code available upon acceptance.

## II. METHOD

Figure 1-A summarizes our architecture. In this section we further define our training procedure, fusion, and attention operations. Each modality  $M_i$  is first encoded by a pretrained and frozen backbone into a modality-specific latent vector  $\mathbf{x}_i \in \mathbb{R}^{d_i}$ . A learnable GW encoder  $E_i : \mathbb{R}^{d_i} \rightarrow \mathbb{R}^d$  maps this latent into a GW representation

$$\mathbf{g}_i = E_i(\mathbf{x}_i) \in \mathbb{R}^d. \quad (1)$$

*Sets definition:* Let  $\mathcal{M} = M_1, \dots, M_n$  be the set of modalities targeted for representation learning. Because samples may have a differing number of views, for a training sample we observe a subset  $\mathcal{M}' \subseteq \mathcal{M}$  (e.g., {image, text} or image only). To fully use the available supervision provided

by matched multimodal samples in the dataset, we compute our losses with all possible input subsets  $\mathcal{M}'' \subseteq \mathcal{M}'$ .

*Fusion:* For any non-empty encoder subset  $\mathcal{M}'' \subseteq \mathcal{M}'$ , we form a fused GW latent

$$\mathbf{z}_{\mathcal{M}''} = f \left( \sum_{M_i \in \mathcal{M}''} \alpha_i \mathbf{g}_i \right), \quad (2)$$

where  $f(\cdot)$  is  $\tanh$  and  $\alpha = (\alpha_i)_{M_i \in \mathcal{M}''}$  is a simplex vector ( $\alpha_i \geq 0$ ,  $\sum_i \alpha_i = 1$ ).

### A. Broadcast operator and set notations

*Broadcast primitive (set-to-set):* Following the spirit of [22], we define a single primitive operation and derive all representation-learning objectives from it. Given a non-empty *input (encoder) subset*  $\mathcal{I} \subseteq \mathcal{M}'$  and a non-empty *output (target) subset*  $\mathcal{O} \subseteq \mathcal{M}'$ , we define the broadcast operator

$$\text{Br}_{\mathcal{I} \rightarrow \mathcal{O}} (\{\mathbf{x}_i\}_{M_i \in \mathcal{I}}) = \{ D_j (f(\sum_{M_i \in \mathcal{I}} \alpha_i E_i(\mathbf{x}_i))) \}_{M_j \in \mathcal{O}}$$

where  $D_j$  is a learnable GW decoder.

*Random fusion during representation learning:* Unless stated otherwise, *all* representation learning objectives in Sec. II-B use *random* fusion weights whenever Eq. (2) is invoked: we sample i.i.d. scores  $s_i \sim \mathcal{U}(0, 1)$  for  $M_i \in \mathcal{M}''$  and set

$$\alpha_i = \frac{\exp(s_i/\tau)}{\sum_{k \in \mathcal{M}''} \exp(s_k/\tau)}.$$

where  $\tau > 0$  is the temperature.

## B. Representation learning objectives

We build on the global latent workspace framework of [22], which optimizes translation, demi-cycle (reconstruction), cycle-consistency, and contrastive alignment between pretrained modules through an amodal shared space. Devillers et al [22] demonstrated the usefulness of each loss component with systematic ablations. They observed that self-supervised losses (e.g. cycle- and demi-cycle-consistency) were important to limit the amount of paired multimodal data required for training; the ability to broadcast GW information to all modules (i.e., using translations and demi-cycles) was also key for efficient representation learning—it enhanced generalization abilities relative to purely contrastive baselines. Our key extension at this step (i.e., aside from the attention mechanism) is that the GW can be written to by *multiple modalities at once* through the fusion operator in Eq. (2). We therefore generalize their one-to-one formulation by expressing objectives as instances of the set-to-set broadcast primitive  $\text{Br}_{\mathcal{I} \rightarrow \mathcal{O}}$  introduced above. In our implementation, for each encoder subset we decode to all modalities in  $\mathcal{M}$ ; as explained below, demi-cycle and translation losses are defined respectively on  $\mathcal{I}$  and  $\mathcal{O}$  subsets of the observed set  $\mathcal{M}'$ , while the cycle-consistency loss makes use of the remaining modalities in  $\mathcal{M} \setminus \mathcal{M}''$ .

Let  $\mathcal{L}_j(\cdot, \cdot)$  be a modality-specific loss (e.g. MSE for continuous latents, BCE for label vectors), and  $M_j$  the ground truth for modality  $j$ , both in backbone latent space.

*Demi-cycle loss:* For any non-empty input subset  $\mathcal{M}'' \subseteq \mathcal{M}'$ , the demi-cycle objective is the self-target special case of the broadcast primitive:

$$\mathcal{L}_{\text{dcy}}^{\mathcal{M}''} = \sum_{M_j \in \mathcal{M}''} \mathcal{L}_j \left( \text{Br}_{\mathcal{M}'' \rightarrow \{M_j\}} (\{\mathbf{x}_i\}_{M_i \in \mathcal{M}''}), \mathbf{x}_j \right) \quad (3)$$

*Translation loss:* Using the same input subset  $\mathcal{M}''$ , the translation objective corresponds to broadcasting to the remaining observed modalities:

$$\mathcal{L}_{\text{tr}}^{\mathcal{M}''} = \sum_{M_j \in \mathcal{M}' \setminus \mathcal{M}''} \mathcal{L}_j \left( \text{Br}_{\mathcal{M}'' \rightarrow \{M_j\}} (\{\mathbf{x}_i\}_{M_i \in \mathcal{M}''}), \mathbf{x}_j \right) \quad (4)$$

*Cycle-consistency loss:* We use a cycle-consistency loss as an unsupervised regularizer inspired by back-translation [24], [25] and adapted to the set-to-set broadcast primitive. For each non-empty input subset  $\mathcal{M}'' \subseteq \mathcal{M}'$ , let  $\overline{\mathcal{M}''} = \mathcal{M} \setminus \mathcal{M}''$  be the complementary modality set (including modalities that may be unknown for that sample). We first broadcast from the inputs  $\mathcal{M}''$  to the complementary set  $\overline{\mathcal{M}''}$ :

$$\{\hat{\mathbf{x}}_j\}_{M_j \in \overline{\mathcal{M}''}} = \text{Br}_{\mathcal{M}'' \rightarrow \overline{\mathcal{M}''}} (\{\mathbf{x}_i\}_{M_i \in \mathcal{M}''}). \quad (5)$$

We then treat these predicted latents as inputs and broadcast back to the original subset  $\mathcal{M}''$ :

$$\{\tilde{\mathbf{x}}_i\}_{M_i \in \mathcal{M}''} = \text{Br}_{\overline{\mathcal{M}''} \rightarrow \mathcal{M}''} (\{\hat{\mathbf{x}}_j\}_{M_j \in \overline{\mathcal{M}''}}), \quad (6)$$

and define the cycle-consistency loss by comparing the reconstructions to the ground truth on the original inputs:

$$\mathcal{L}_{\text{cycle}}^{\mathcal{M}''} = \sum_{M_i \in \mathcal{M}''} \mathcal{L}_i (\tilde{\mathbf{x}}_i, \mathbf{x}_i) \quad (7)$$

*Contrastive alignment loss:* We additionally align modality representations in the prefusion GW space using a pairwise contrastive loss  $\mathcal{L}_{\text{contrast}}$  (InfoNCE) over modalities in  $\mathcal{M}'$ .

*Overall representation learning objective:* We optimize a weighted sum of translation, demi-cycle, cycle-consistency, and contrastive alignment losses:

$$\mathcal{L}_{\text{rep}} = \lambda_{\text{tr}} \mathcal{L}_{\text{tr}} + \lambda_{\text{dcy}} \mathcal{L}_{\text{dcy}} + \lambda_{\text{cycle}} \mathcal{L}_{\text{cycle}} + \lambda_{\text{contrast}} \mathcal{L}_{\text{contrast}} \quad (8)$$

with  $\lambda_{\text{tr}}, \lambda_{\text{dcy}}, \lambda_{\text{cycle}}, \lambda_{\text{contrast}} \geq 0$ .

## C. Top-down modality attention

Our attention mechanism replaces the random fusion weights  $\alpha$  in Eq. (2) with *data-dependent* modality weights. It computes a query from a fused GW state, and compares it to modality-specific keys derived from the pre-fusion GW latents.

Given pre-fusion latents  $\{\mathbf{g}_i\}_{M_i \in \mathcal{M}''}$ , we use linear maps  $K, Q : \mathbb{R}^d \rightarrow \mathbb{R}^h$  (with  $K$  shared across modalities) to form

$$\mathbf{k}_i = K(\mathbf{g}_i) \in \mathbb{R}^h, \quad \mathbf{q} = Q(\mathbf{z}^{\text{init}}) \in \mathbb{R}^h.$$

Since the query depends on a fused GW state, we first initialize it with uniform weights:

$$\alpha_i^{(\text{init})} = \frac{1}{|\mathcal{M}''|}, \quad \mathbf{z}^{(\text{init})} = f \left( \sum_{M_i \in \mathcal{M}''} \alpha_i^{(\text{init})} \mathbf{g}_i \right).$$

And lastly, we score each modality by dot-product similarity to the query and normalize across modalities:

$$\ell_i = \langle \mathbf{k}_i, \mathbf{q} \rangle, \quad \alpha_i = \text{softmax}_{i \in \mathcal{M}''} (\ell_i)$$

## III. EXPERIMENTAL SETUP

### A. Datasets

1) *Simple Shapes:* First, we evaluate our approach on a synthetic dataset from [22], the Simple Shapes Dataset. Samples from this dataset are geometric shapes (diamonds, triangles, eggs) with a given size, position, color, and rotation. They can be described in three modalities : text, images, and attribute vectors (the latter being a complete numerical description of the sample). The dataset comprises 1 million samples at train time, 50,000 for validation and 1000 at test time. This version of the dataset is used to pretrain the modality-specific backbones and the GW multimodal representation with the representation learning objectives described in Section II-B.

We define 5 downstream classification tasks, one for each of the 5 attributes in the Simple Shapes Dataset. Only one of the four attributes is categorical so we thus build a second, restricted dataset specifically for training and testing classification heads. In it, we only use 9 different RGB values. For rotation, we separate the circle into 16 bins of width  $\pi/8$ , and only keep samples inside the 4 bins corresponding to top, bottom, left and right. For the position attribute, we split the 2D space into  $7 \times 7$  bins (integer x and y positions between  $[-3, 3]$ ), and keep only samples inside four chosen

bins: bottom  $(x, y) = (0, -2)$ , top  $(0, 2)$ , left  $(-2, 0)$  and right  $(0, 2)$ . Lastly, for size, we use 4 non-overlapping bins that cover the entirety of possible sizes. This makes the classification tasks intrinsically easy (for in-distribution, clean data samples), allowing us to focus our experiments on noise-robustness. For this classification dataset, we have 500,000 train samples, and 1,000 for testing.

2) *MM-IMDb 1.0*: The second dataset we use is MM-IMDb 1.0 [9]. It is an ideal choice for our experiments: movie synopses (text) and posters (image) are used to classify the genre of each movie (label). The text and image sometimes provide redundant but sometimes conflicting information, and are not always equally informative. The dataset consists of 15,552 train movies, 2,608 for validation, and 7,799 for test, each represented by its synopsis (text) and poster (image). We use binary labels (across 23 distinct but not mutually exclusive genres), both as a third input modality (when training our GW architecture for multimodal representation objectives), and as a classification target (when training the attention selection mechanism; in this case, labels are never provided as inputs).

In both datasets, we encode all the samples through frozen pretrained backbones (acting as the “modules” of our GW architecture), and use these latent vectors as our GW inputs.

## B. Reproducibility details

1) *Simple Shapes*: On Simple-Shapes, we use *simple-shapes-pretrained* VAEs as frozen backbones for images and attributes (latent sizes 8 and 10 respectively), and a pretrained RNN for text (one latent vector of size 64 per sample). For the Global Workspace (GW), we use a latent dimension  $d = 32$  and implement each GW encoder/decoder as an MLP with two hidden layers of size 64. Classification probes are 4-layer MLPs with hidden size 512, batch normalization, dropout  $p = 0.2$ , and GELU activations. Our modality attention uses linear Key and Query projections with head size  $h = 64$ . We use a batch size of 512. Training: The GW is trained for 100,000 steps with Adam and a OneCycleLR schedule, using loss coefficients  $\lambda_{\text{tr}} = \lambda_{\text{cycle}} = \lambda_{\text{dce}} = 1$  and  $\lambda_{\text{contrast}} = 0.01$ . The GW is then frozen, while classification probes are trained for 3 epochs. Finally, with frozen probes, attention is trained for 5 epochs.

2) *MM-IMDb 1.0*: On MM-IMDb, we treat the labels (movie genres) as a third modality during GW multimodal representation learning. GW encoders and decoders are 4-hidden-layer MLPs of width 384, with residual connections skipping the first two hidden layers and skipping the last two hidden layers. Our modality attention uses linear Key and Query projections with head size  $h = 256$ . We use the same loss coefficients as in the Simple Shapes case.

**For the corruption robustness tests** : We pretrain the GW multimodal representation on labels, images and text without augmentations. The GW is then frozen during classification probe training and attention training. We encode the synopsis text and poster images with *BAAI/bge-base-en-v1.5* and *facebook/dinov2-base* respectively, using the CLS token.

**For the performance comparison benchmark** : We adopt the same data augmentation scheme as [23]: default SimCLR augmentations for images and BERT-style token masking for text. We use the same backbones : CLIP (*openai/clip-vit-base-patch32* for images; *sentence-transformers/clip-ViT-B-32-multilingual-v1* for text) and/or BLIP-2 (*Salesforce/blip2-flan-t5-xl*). We average-pool the backbone output tokens along the sequence dimension to obtain a single latent vector per sample. Using augmentation allows joint pretraining of the attention mechanism with the GW: for the broadcast loss, we feed augmented inputs to the encoders while decoders predict non-augmented (“clean”) targets. We train the attention mechanism only when image and text are jointly provided as the input partition; for all other input partitions we use random fusion scores, as in the Simple Shapes case.

## IV. RESULTS

### A. Noise Robustness on Simple Shapes and MM-IMDb

We follow a multi-stage training procedure. First, we train the global workspace on the three modalities using clean data from the original dataset. Then, in the Simple Shapes case, we train one probe per classification task, with the global workspace frozen, still on clean data. For MM-IMDb, we train one probe for all the labels. During probe and GW training, we uniformly sample selection scores for each modality, and apply a softmax across modalities before fusing them into the GW representation. We then keep the GW and classification probes frozen while training the attention mechanism.

First, we aim to show that our attentional system can learn to select modalities so as to improve performance on a downstream task. To test this, during both training and evaluation we randomly, per-sample, pick two out of the three modalities and add corruption to their latent vectors. On Simple Shapes, the corruption is Gaussian noise, with different possible standard deviations. On MM-IMDb, to approximate realistic distribution shifts, we use the image and text corruption methods proposed in [3], with the severity parameter always set to 5 (most severe), and apply between 1 and 4 corruptions at once to manipulate task difficulty. In our setting, maximum noise on Simple Shapes leads to chance level performance (23 percent), and on MM-IMDb, 4 corruptions being applied leads to a 7 percent drop in performance.

As baselines, we use GMU [9] and DynMM [11]. We choose GMU (a classic feature-wise attention mechanism) to assess whether feature-wise attention could surpass our method by tuning out the features corresponding to the noise. DynMM applies a gating (soft during training, hard during testing) mechanism between multiple possible fusion methods: average, max, concatenation followed by a linear layer, and choice of either modality alone. We use it as a baseline because its attention mechanism can learn to use a single score per modality if it chooses the single-modality options. Both baselines are finetuned end-to-end on the classification tasks, with noised inputs. This means that, unlike us, all of their parameters (including encoders and probes) are directly optimized for noise robustness (see Table I).

TABLE I  
PARAMETER COUNTS FOR THE SIMPLE SHAPES AND MM-IMDb 1.0 TRAINING SETUPS.

Model	Params	Trained on Labels	Trained with Corruption	Pretrained (backbones)
<i>Simple Shapes</i>				
GMU	113,340	113,340	113,340	2,981,946
DynMM	92,578	92,578	92,578	2,981,946
Ours	68,764	64,220	4,544	3,082,540
<i>MM-IMDb 1.0</i>				
DynMM	4.48M	4.48M	4.48M	196.06M
GMU	5.01M	5.01M	5.01M	196.06M
GW	7.98M	4.02M	0.06M	204.68M

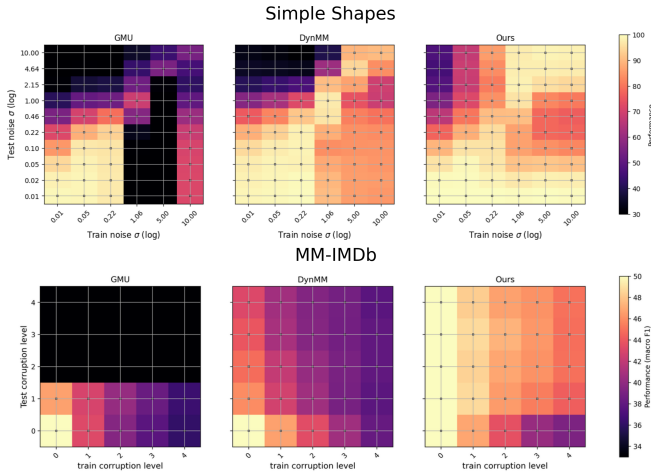


Fig. 2. Simple Shapes (top): accuracy heatmaps for GMU, DynMM, and our method across train noise  $\sigma$  (columns) and test noise  $\sigma$  (rows), averaged over tasks and corrupted-modality choices. MM-IMDb (bottom): macro-F1 heatmaps across train and test corruption levels, averaged over tasks and corruption types.

In figure 2, we observe that all models struggle when trained on a certain corruption level and evaluated on a different level. Still, although our probes and Global Workspace encoders have never encountered any corruption, our model holds up well for in-distribution levels of noise, and outperforms the other models for most out-of-distribution noise levels. On Simple Shapes, for instance, our attention system trained with only  $\approx 4,000$  parameters (see table I) can better adapt to new input statistics than dedicated attention systems trained with 20-25 times more parameters. But can the attention mechanism also generalize to unseen classification tasks, or unseen modalities? We explore this in the next section.

### B. Generalization across tasks and modalities

*Leave-out task:* We argue that one of the advantages of our GW implementation is more flexible processing. This could manifest as the ability to learn behavior on one task, and transfer it to the next without retraining attention parameters. On Simple Shapes, to put this to the test, we start from a pretrained GW and 5 classification probes trained on clean data, just as in the previous experiment. We then introduce

the same noise schedule to train the attention mechanism, but only on one of the 5 tasks. At inference, we test this attention mechanism on the 4 other probes. In all the following generalization tests, we set the noise standard deviation to  $\sigma = 5$  for both training and evaluation, a high level ensuring that the task can only be solved by tuning out the noise.

We also test our hypothesis on the more realistic MM-IMDb with our realistic corruptions. We divide the target labels into 4 arbitrary subsets; predicting one subset of labels with the pretrained probe corresponds to a *task*. We use the maximum level of corruption (4). As before, we train our attention mechanism on one task, and test it on the 3 other probes.

As baselines, we train DynMM and GMU systems end-to-end on a single classification task, freeze their encoders and fusion mechanisms, and train new probes for the left-out tasks, using the frozen fused representation. Additionally, we also measure the performance of our GW (and classification probes) in the same conditions but without attention, i.e. with random fusion scores.

The results for our leave-out generalization tests are shown in figure 3. Our GW attention generalizes nearly perfectly to the left-out tasks, owing to the generality of the learned representation in our multi-stage training paradigm. The attention mechanism has never seen the left-out tasks, and the probes and GW have never seen the corruption; nonetheless, the attention system is able to use one task scenario to learn the signatures of reliable vs. unreliable modalities, in a way that can generalize to other tasks scenarios. In contrast, other attention systems (DynMM and GMU) learn task- and corruption-specific strategies that do not transfer well to out-of-distribution settings. Having validated that our representation and attention methods can transfer knowledge from task to task, we now ask if they can learn a strategy for one modality and apply it to another.

*Modality-wise generalization I: unseen clean modality:* Can our attention mechanism apply knowledge learned on two modalities to the third one? To test this, we change the noise schedule so that one of the three modalities is never provided as clean during training (as before, only one modality can be clean at a time). We expect the trained attention system to assign a low or negligible weight to this modality. At inference, we go back to the normal noising schedule where any modality can be clean; will the trained attention system be able to assign a high weight to the previously left-out modality when it is the only clean one? As this test requires at least 3 modalities, it can only be performed for the simple-shapes-dataset.

As baselines, we include GMU and DynMM, training them end-to-end on the new restricted noise schedule, and evaluating on the normal noise schedule. Since these two methods normally train their probes in the final noisy conditions, we finetune the classification probes (but not the rest of the attention systems) on the normal noise schedule before testing. As always, we also include the GW random fusion baseline, i.e. our model without attention.

In figure 4, we see that for our model, removing the constraint on the “always-noised” modality at inference time

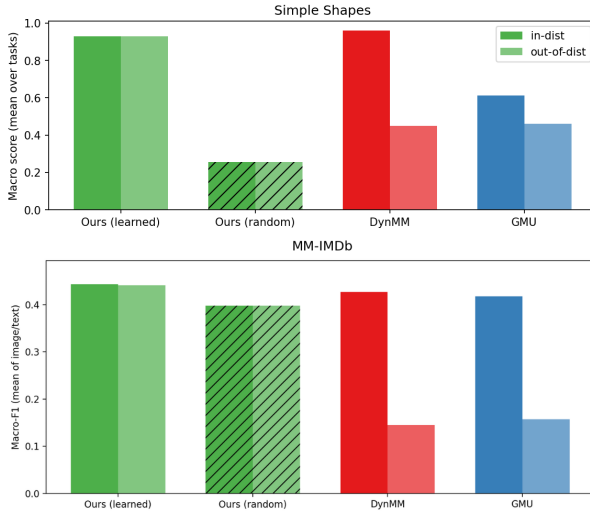


Fig. 3. In- vs. out-of-distribution leave-out generalization on Simple-Shapes and MM-IMDb. For each model, we report performance when the training task matches the evaluation task (in-distribution) versus when it differs (out-of-distribution) respectively. Results are averaged on 3 seeds.

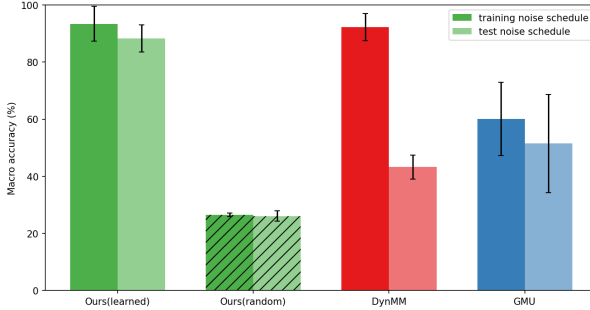


Fig. 4. Modality generalization test I: unseen clean modality. The systems are trained on all 5 classification tasks at once, with one of the 3 modalities always noised. For each model, the first bar represents accuracy under training conditions, and the second reflects test-time accuracy, where the left-out modality can be the one shown without noise. The bars correspond to average performance across all 3 possible left-out modalities, and all 5 tasks. For GMU and DynMM, we fine-tuned the classification probes on the new noise distribution before testing. Despite this fine-tuning, the systems could not generalize well to the new situation (hashed bars). For Our model, no fine-tuning was necessary (since the probes are always trained on clean inputs). Yet, our model could generalize well, and outperform the other baselines (but only using a trained attention strategy, not with random modality scores).

results in less than 5 percent accuracy drop. In contrast, performance for the random fusion baseline collapses. Thus, our system was able to learn efficient key and query matrix weights from one modality, and apply them to another without retraining.

On the contrary, for GMU and DynMM baselines, performance is much lower when changing the noise schedule, because they are trained end-to-end on one configuration and struggle to transfer their learned strategy to an unseen configuration. In this test, we aimed to leave out one modality from attention training by always noising it; next, we attempt to actually leave out one of the 3 modalities.

TABLE II  
MM-IMDb 1.0 MACRO-F1. FOR CLIP, BLIP-2, CoMM AND MFAS, WE DRAW PERFORMANCE VALUES FROM [23]. FOR GMU AND BRIDGETOW, WE USE VALUES FROM [26]. BY “END-TO-END” WE MEAN THE ENTIRE MODEL WAS TRAINED OR FINE-TUNED DIRECTLY ON THE FINAL CLASSIFICATION OBJECTIVE.

Model	Macro-F1	End-to-end	Train FLOPs (est.)
GMU (Arevalo et al., 2017)	54.10	yes	–
MFAS [27]	55.60	yes	–
CoMM (CLIP, finetuned)	58.97±0.19	yes	–
CoMM (BLIP-2, finetuned)	62.00±0.25	yes	$> 4.7 \cdot 10^{15}$
BridgeTow [28]	63.30	–	–
BLIP-2 [29]	49.90	no	–
CLIP [30]	50.90	no	–
Ours (GW, CLIP, random)	50.00±1.99	no	–
Ours (GW, CLIP)	53.48±0.37	no	–
CoMM (CLIP, linear readout) [23]	54.63±0.22	no	–
CoMM (BLIP-2, linear readout)	58.44±0.43	no	$4.7 \cdot 10^{15}$
Ours (GW, BLIP-2, random)	60.41±0.52	no	$7.5 \cdot 10^{14}$
Ours (GW, BLIP-2)	65.34±0.14	no	$7.5 \cdot 10^{14}$

*Modality-wise generalization II: unseen modality:* As a second, stronger modality generalization task, we start once again from the frozen GW and classification probes trained on clean data. Then, we leave out one of the modalities completely during attention training. Since there are only two modalities left, we adapt the training noise schedule to have only one noisy and one clean modality, randomly determined on each sample. Then at inference, we add the left-out modality back (with 2 randomly assigned clean modality and 1 noisy one), and test whether the attention mechanism is able to recognize when this left-out modality is clean vs. noisy, and select it or tune it out (respectively). For this experiment, we cannot include GMU and DynMM as baselines, because their gating mechanisms are designed for a fixed number of modalities. In our case, as the key layer is shared across modalities, our attentional mechanism can be flexibly extended to new modalities. To validate this transfer capability, we use random fusion scores as a no-attention baseline.

Figure 5 shows that our attention system is indeed able to generalize to an additional modality : adding a third modality actually increases performance, because now only one of three modalities is noised (instead of one of two during training). In contrast, we see that adding a third modality only slightly increases performance for the random variant, meaning that the noise corruption remains a challenging test, even when two clean modalities are present instead of one. In addition, we analyze the attention scores given to the left-out modality, compared to the trained modalities. We see that the trained attention strategy extends almost perfectly to the left-out, unseen modality. This is made possible by the amodal representation learned with our broadcast loss, combined with the sharing of the key matrix across modalities.

### C. MM-IMDB 1.0 benchmark

Our attention mechanism proved helpful in terms of robustness to corrupted modalities and generalization to out-of-distribution conditions. We now want to see how it performs

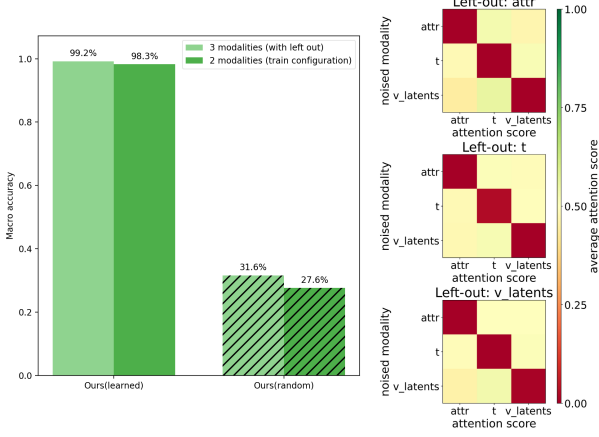


Fig. 5. Modality generalization test II: unseen modality. We train the attention system on two and test on three modalities. **Left** : Our attention mechanism’s performance vs. random fusion performance (no-attention), under both train and evaluation configurations. The bars show accuracy averaged across 3 possible left-out modalities, 5 tasks, and all combinations of noisy/clean modalities. **Right** : average attention scores given by our attention mechanism on the test dataset, as a function of the noised modality. We show results separately for each left-out modality, and notice that attention scores on the left-out modality are comparable to trained modalities: this means our attention mechanism perfectly generalizes to the left-out modality.

on a more standard multimodal integration benchmark, where informative modalities are defined by potentially more subtle cues than the presence or absence of corruptions. We thus use the MM-IMDb 1.0 benchmark (without any corruption) for this purpose. This time, we train our attention mechanism alongside the global workspace, so that it can directly learn to facilitate multimodal integration (rather than noise- or corruption-robustness). Because we train a 3-modality Global Workspace with the labels as a modality, we don’t need a classification probe to predict labels after training—we simply use the trained labels decoder.

To contextualize our performance on the MM-IMDb benchmark, we include multiple baselines from the literature, ranging from representation learning methods [23], [28], [30], to task-oriented, end-to-end methods [1], [9]. In an effort to best compare our model with these baselines, we train two versions of the GW, using either BLIP2 or CLIP as backbones (as done for the CoMM model). As an ablation to check that our attention mechanism is actually useful, we also include the random attention scores version of our method, where no attention is used during GW training.

Results are reported in table II. Although our model’s BLIP2 variant has the highest score overall, direct comparison between all these very different methods should be made with caution. For starters, while the best CoMM model is finetuned end-to-end for label classification, in their pretraining step they do not use the labels as we do. BridgeTow uses a general representation trained on millions of image-text samples, then adapted to the very particular domain of MM-IMDb, which can limit its performance if movie posters or synopses are too far out of the training distribution. However, the purpose of this experiment is not to claim that our method is superior

to all others, but only that it can perform well on a real-data, competitive benchmark. Furthermore, the results clearly reveal the usefulness of our attention mechanism, with a 5-point increase over the no-attention GW variant (random) using the BLIP2 backbone.

We note that using the CLIP backbone, GW performance is much worse than with BLIP2. We can attribute this difference to average-pooling of the backbone tokens along the sequence dimension, which reduces the backbone output to a single 512-dimensional vector in the CLIP case—much more restrictive than BLIP2’s 2048 dimensions. CoMM does not have such a performance gap between the two backbones, because they fuse modalities through a transformer that makes use of all the available tokens.

Beyond classification performance, we also consider the computational efficiency of our model and training procedure in table II. We find that our model is efficient when compared with CoMM, requiring significantly less floating-point operations to train, while using approximately the same number of parameters.

## V. ACKNOWLEDGEMENTS

This work was supported by the French Agence Nationale de la Recherche via an ANITI Chair (ANITI ANR-19-P3IA-0004 and ANITI AI Cluster ANR-23-IACL-0002), an ANR grant COCOBOT (ANR21- FAI2-0005) and by “Défi Clé Robotique centrée sur l’humain” funded by Région Occitanie, France. This research is also funded by the European Union (ERC Advanced GLOW project number 101096017). Views and opinions expressed are however those of the authors only and do not necessarily reflect those of the European Union or the European Research Council Executive Agency. Neither the European Union nor the granting authority can be held responsible for them

## VI. DISCUSSION

GWT provides a framework for flexible multimodal integration in AI systems. Prior work has revealed the potential of this framework for downstream classification tasks [22] or for cross-modal transfer in RL agents [20], [21]. In this work, we proposed a possible implementation for an attention controller in a Global Workspace architecture, and explored its properties. A combination of supervised (contrastive, translation) and unsupervised losses (cycles, demi-cycles), allows us to learn a fused, amodal GW representation. We complement this architecture with an attention mechanism that optimally selects the input modalities; depending on the application, this attention mechanism can be trained along with the global workspace for representation learning objectives, or separately for a specific downstream task.

On a synthetic dataset of geometric shapes and on the more naturalistic MM-IMDb 1.0 dataset, we demonstrated that training the attention mechanism with a frozen GW representation makes the system more robust to corruption than baselines from the literature. The attention system focused the multimodal fusion weights on the clean modality and ignored

the corrupted one(s). We also found that our system could generalize to new, out-of-distribution conditions, whether of noise patterns, of unseen downstream tasks, or even unseen modalities, without any finetuning.

We then tested our system with end-to-end training on the multimodal MM-IMDB benchmark, and reported high performance as well as high training efficiency. With increases in performance compared to a no-attention baseline, the usefulness of the attention mechanism was evident: for some movies, more attention was focused on the poster, for others on the text synopsis, and as a result, the GW was better at predicting the movie genre label.

However, some limitations remain to be addressed in future work. First, all tasks considered in this work involve purely static data, whereas many multimodal applications could benefit from dynamic processing (e.g. video and audio). While dynamical data is outside the scope of this work, our attention mechanism (Figure 1B) can in principle operate iteratively over multiple time steps. Dynamical processing could thus be the logical next goal for our GW system.

Second, the only modalities tested here are images and text (with Simple-shapes attribute vectors or MM-IMDb labels constituting a sort of proto-linguistic representation). But the architecture presented in this work could, in theory, scale to any number of modalities (sound, infrared sensors, etc.). This is another promising future avenue.

## REFERENCES

- [1] T. Baltrušaitis, C. Ahuja, and L.-P. Morency, “Multimodal machine learning: A survey and taxonomy,” *IEEE Transactions on Pattern Analysis and Machine Intelligence*, vol. 41, no. 2, pp. 423–443, 2019.
- [2] R. Wu, H. Wang, H.-T. Chen, and G. Carneiro, “Deep multimodal learning with missing modality: A survey,” *arXiv preprint arXiv:2409.07825*, 2024.
- [3] J. Qiu, Y. Zhu, X. Shi, F. Wenzel, Z. Tang, D. Zhao, B. Li, and M. Li, “Benchmarking robustness of multimodal image-text models under distribution shift,” 2024, *arXiv:2212.08044v3 [cs.CV]*. Accepted by Journal of Data-centric Machine Learning Research (DMLR) 2024. [Online]. Available: <https://arxiv.org/abs/2212.08044>
- [4] J. Ngiam, A. Khosla, M. Kim, J. Nam, H. Lee, and A. Y. Ng, “Multimodal deep learning,” in *Proceedings of the 28th International Conference on Machine Learning (ICML-11)*. Bellevue, Washington, USA: Omnipress, 2011, pp. 689–696.
- [5] N. Neverova, C. Wolf, G. W. Taylor, and F. Nebout, “Moddrop: Adaptive multi-modal gesture recognition,” *IEEE Transactions on Pattern Analysis and Machine Intelligence*, vol. 38, no. 8, pp. 1692–1706, 2016. [Online]. Available: <https://doi.org/10.1109/TPAMI.2015.2461544>
- [6] M. Ma, J. Ren, L. Zhao, S. Tulyakov, C. Wu, and X. Peng, “Smil: Multimodal learning with severely missing modality,” in *Proceedings of the AAAI Conference on Artificial Intelligence*, vol. 35, no. 3, 2021, pp. 2302–2310.
- [7] E. Strubell, A. Ganesh, and A. McCallum, “Energy and policy considerations for deep learning in NLP,” in *Proceedings of the 57th Annual Meeting of the Association for Computational Linguistics*. Association for Computational Linguistics, 2019, pp. 3645–3650.
- [8] R. Bommasani, D. A. Hudson, E. Adeli, R. Altman, S. Arora, S. von Arx, M. S. Bernstein, J. Bohg, A. Bossetut, E. Brunskill *et al.*, “On the opportunities and risks of foundation models,” *arXiv preprint arXiv:2108.07258*, 2021.
- [9] J. Arevalo, T. Solorio, M. Montes-y-Gómez, and F. A. González, “Gated multimodal units for information fusion,” *arXiv preprint*, 2017, introduces the GMU and releases the MM-IMDb dataset.
- [10] Y.-H. H. Tsai, S. Bai, P. P. Liang, J. Z. Kolter, L.-P. Morency, and R. Salakhutdinov, “Multimodal transformer for unaligned multimodal language sequences,” in *Proceedings of the 57th Annual Meeting of the Association for Computational Linguistics*. Florence, Italy: Association for Computational Linguistics, July 2019, pp. 6558–6569. [Online]. Available: <https://aclanthology.org/P19-1656/>
- [11] Z. Xue, L. Chen, Y. Wei, L. Wang, and X. Chen, “Dynamic multimodal fusion (dynmm),” in *Proceedings of the IEEE/CVF Conference on Computer Vision and Pattern Recognition Workshops (CVPRW)*, 2023. [Online]. Available: [https://openaccess.thecvf.com/content/CVPR2023W/MULA/papers/Xue\\_Dynamic\\_Multimodal\\_Fusion\\_CVPRW\\_2023\\_paper.pdf](https://openaccess.thecvf.com/content/CVPR2023W/MULA/papers/Xue_Dynamic_Multimodal_Fusion_CVPRW_2023_paper.pdf)
- [12] B. J. Baars, *A Cognitive Theory of Consciousness*. Cambridge; New York: Cambridge University Press, 1988.
- [13] S. Dehaene, M. Kerszberg, and J.-P. Changeux, “A neuronal model of a global workspace in effortful cognitive tasks,” *Proceedings of the National Academy of Sciences*, vol. 95, no. 24, pp. 14 529–14 534, 1998.
- [14] S. Dehaene, J. Changeux, and L. Naccache, “The global neuronal workspace model of conscious access: From neuronal architectures to clinical applications,” in *Characterizing Consciousness: From Cognition to the Clinic?*, ser. Research and Perspectives in Neurosciences, S. Dehaene and Y. Christen, Eds. Berlin, Heidelberg: Springer, 2011, pp. 55–84.
- [15] R. VanRullen and R. Kanai, “Deep learning and the global workspace theory,” *Trends in Neurosciences*, vol. 44, no. 9, pp. 692–704, 2021.
- [16] C. Bao, Z. Fountas, T. Olugbade, and N. Bianchi-Berthouze, “Gwn: Multimodal data fusion based on the global workspace via hierarchical skip connections and multi-head attention,” in *Proceedings of the 2020 International Conference on Multimodal Interaction (ICMI ’20)*, 2020.
- [17] A. Goyal, A. Didolkar, A. Lamb, K. Badola, N. R. Ke, N. Rahaman, J. Binas, C. Blundell, M. C. Mozer, and Y. Bengio, “Coordination among neural modules through a shared global workspace,” *arXiv preprint arXiv:2103.01197*, 2021. [Online]. Available: <https://arxiv.org/abs/2103.01197>
- [18] Y. Sun, “Associative transformer,” in *Proceedings of the IEEE/CVF Conference on Computer Vision and Pattern Recognition (CVPR)*, 2025. [Online]. Available: [https://openaccess.thecvf.com/content/CVPR2025/papers/Sun\\_Associative\\_Transformer\\_CVPR\\_2025\\_paper.pdf](https://openaccess.thecvf.com/content/CVPR2025/papers/Sun_Associative_Transformer_CVPR_2025_paper.pdf)
- [19] R. F. J. Dossa, M. Methnani *et al.*, “Design and evaluation of a global workspace agent embodied in a realistic multimodal environment,” *Frontiers in Computational Neuroscience*, 2024. [Online]. Available: <https://pmc.ncbi.nlm.nih.gov/articles/PMC11211627/>
- [20] L. Maytié, B. Devillers, A. Arnold, and R. VanRullen, “Zero-shot cross-modal transfer of Reinforcement Learning policies through a global workspace,” *Reinforcement Learning Journal*, vol. 3, pp. 1410–1426, Mar. 2024, presented at the Reinforcement Learning Conference (RLC), Amherst, MA, Aug. 9–12, 2024. [Online]. Available: <https://arxiv.org/abs/2403.04588>
- [21] L. Maytié, R. Bertin Johannet, and R. VanRullen, “Multimodal dreaming: A global workspace approach to world model-based Reinforcement Learning,” Feb. 2025. [Online]. Available: <https://arxiv.org/abs/2502.21142>
- [22] B. Devillers, L. Maytié, and R. VanRullen, “Semi-supervised multimodal representation learning through a global workspace,” *IEEE Transactions on Neural Networks and Learning Systems*, vol. 36, no. 5, pp. 7843–7857, 2025.
- [23] B. Dufumier, J. Castillo-Navarro, D. Tuia, and J.-P. Thiran, “What to align in multimodal contrastive learning?” in *Proceedings of the International Conference on Learning Representations (ICLR)*, 2025, poster. [Online]. Available: <https://openreview.net/forum?id=Pe3AxLq6Wf>
- [24] M. Artetxe, G. Labaka, E. Agirre, and K. Cho, “Unsupervised neural machine translation,” *arXiv preprint*, 2017, published as a conference paper at ICLR 2018. [Online]. Available: <https://arxiv.org/abs/1710.11041>
- [25] G. Lample, M. Ott, A. Conneau, L. Denoyer, and M. Ranzato, “Phrase-based & neural unsupervised machine translation,” *arXiv preprint*, 2018, eMNL 2018. [Online]. Available: <https://arxiv.org/abs/1804.07755>
- [26] J. Li, G. Qi, C. Zhang, Y. Chen, Y. Tan, C. Xia, and Y. Tian, “Incorporating domain knowledge graph into multimodal movie genre classification with self-supervised attention and contrastive learning,” in *Proceedings of the 31st ACM International Conference on Multimedia (MM ’23)*. New York, NY, USA: Association for

Computing Machinery, Oct. 2023, pp. 3337–3345. [Online]. Available: <https://dl.acm.org/doi/10.1145/3581783.3612085>

[27] J.-M. Pérez-Rúa, V. Vielzeuf, S. Pateux, M. Baccouche, and F. Jurie, “Mfas: Multimodal fusion architecture search,” in *Proceedings of the IEEE/CVF Conference on Computer Vision and Pattern Recognition (CVPR)*, June 2019, pp. 6966–6975. [Online]. Available: [https://openaccess.thecvf.com/content\\_CVPR\\_2019/papers/Perez-Rua\\_MFAS\\_Multimodal\\_Fusion\\_Architecture\\_Search\\_CVPR\\_2019\\_paper.pdf](https://openaccess.thecvf.com/content_CVPR_2019/papers/Perez-Rua_MFAS_Multimodal_Fusion_Architecture_Search_CVPR_2019_paper.pdf)

[28] S. Huang, L. Dong, W. Wang, Y. Hao, S. Singhal, S. Ma, T. Lv, L. Cui, O. K. Mohammed, B. Patra, Q. Liu, K. Aggarwal, Z. Chi, J. Bjorck, V. Chaudhary, S. Som, X. Song, and F. Wei, “Language is not all you need: Aligning perception with language models,” *arXiv preprint arXiv:2302.14045*, 2023. [Online]. Available: <https://arxiv.org/abs/2302.14045>

[29] J. Li, D. Li, S. Savarese, and S. Hoi, “BLIP-2: Bootstrapping language-image pre-training with frozen image encoders and large language models,” in *Proceedings of the 40th International Conference on Machine Learning*, ser. Proceedings of Machine Learning Research, A. Krause, E. Brunskill, K. Cho, B. Engelhardt, S. Sabato, and J. Scarlett, Eds., vol. 202. PMLR, 23–29 Jul 2023, pp. 19730–19742. [Online]. Available: <https://proceedings.mlr.press/v202/li23q.html>

[30] A. Radford, J. W. Kim, C. Hallacy, A. Ramesh, G. Goh, S. Agarwal, G. Sastry, A. Askell, P. Mishkin, J. Clark, G. Krueger, and I. Sutskever, “Learning transferable visual models from natural language supervision,” in *Proceedings of the 38th International Conference on Machine Learning*, ser. Proceedings of Machine Learning Research, M. Meila and T. Zhang, Eds., vol. 139. PMLR, 18–24 Jul 2021, pp. 8748–8763. [Online]. Available: <https://proceedings.mlr.press/v139/radford21a.html>